JOURNAL OF GEOPHYSICAL RESEARCH, VOL. 111, C06023, doi:10.1029/2005JC003361, 2006

Application of the convolution formalism to the ocean tide potential: Results from the Gravity Recovery and Climate Experiment (GRACE)

S. D. Desai[1] and D.-N. Yuan[1]

Received 20 October 2005; revised 26 January 2006; accepted 24 March 2006; published 17 June 2006.

[1] A computationally efficient approach to reducing omission errors in ocean tide potential models is derived and evaluated using data from the Gravity Recovery and Climate Experiment (GRACE) mission. Ocean tide height models are usually explicitly available at a few frequencies, and a smooth unit response is assumed to infer the response across the tidal spectrum. The convolution formalism of Munk and Cartwright (1966) models this response function with a Fourier series. This allows the total ocean tide height, and therefore the total ocean tide potential, to be modeled as a weighted sum of past, present, and future values of the tide-generating potential. Previous applications of the convolution formalism have usually been limited to tide height models, but we extend it to ocean tide potential models. We use luni-solar ephemerides to derive the required tide-generating potential so that the complete spectrum of the ocean tide potential is efficiently represented. In contrast, the traditionally adopted harmonic model of the ocean tide potential requires the explicit sum of the contributions from individual tidal frequencies. It is therefore subject to omission errors from neglected frequencies and is computationally more intensive. Intersatellite range rate data from the GRACE mission are used to compare convolution and harmonic models of the ocean tide potential. The monthly range rate residual variance is smaller by 4–5%, and the daily residual variance is smaller by as much as 15% when using the convolution model than when using a harmonic model that is defined by twice the number of parameters.

Citation: Desai, S. D., and D.-N. Yuan (2006), Application of the convolution formalism to the ocean tide potential: Results from the Gravity Recovery and Climate Experiment (GRACE), *J. Geophys. Res.*, *111*, C06023, doi:10.1029/2005JC003361.

1. Introduction

[2] Improvements to models of the short period variations in the geopotential, and in particular those with periods of less than two months, will translate into improved accuracies in the monthly gravity fields that are being derived from the Gravity Recovery and Climate Experiment (GRACE) mission. The continually improving accuracy in the precise orbit determination solutions of Earth orbiters may also benefit from these improved models. We focus on reducing omission errors in models of the contribution of the ocean tides to the geopotential, namely the ocean tide potential models. The approach presented in this paper efficiently models the complete spectrum of the ocean tide potential by applying the tide-generating potential (TGP) as computed from luni-solar ephemerides to the convolution formalism of *Munk and Cartwright* [1966], hereinafter referred to as MC66.

[3] The goal of the GRACE mission is to recover the global gravity field at monthly intervals to enable investigation of time variable gravity. Preliminary results indicate that the accuracy of the initial monthly GRACE gravity fields have not achieved the baseline performance goals [e.g., *Wahr et al.*, 2004]. Nevertheless, the accuracy of the initial static gravity fields recovered from GRACE [*Tapley et al.*, 2004b] are more than an order of magnitude better than the previously best available fields, such as EGM96 [*Lemoine et al.*, 1998]. Improvements to the GRACE gravity fields are expected from reprocessing with revised algorithms and models, and from improvements to the on board software [*Tapley et al.*, 2004a]. Unmodeled mass variations with periods shorter than two months will alias into the monthly time series and may contaminate the longer period climatic signals that GRACE is intended to observe [e.g., *Thompson et al.*, 2004]. The ocean tides primarily have periods of 12 and 24 hours so reducing errors in the ocean tide potential models will mitigate errors in both the static and monthly GRACE gravity fields.

[4] The deformations of the Earth that are caused by luni-solar tidal forces provide the largest contribution to temporal variations in the geopotential. The variations from the body tides, or deformations that are caused by the direct effect of the tidal forces on the solid Earth, are accurately modeled by applying Earth models to the TGP [e.g., *McCarthy and Petit*, 2004]. Modeling the variations from the ocean tides, or respective displacements of the oceans, is not as straightforward because the oceans have a significant

[1]Jet Propulsion Laboratory, California Institute of Technology, Pasadena, California, USA.

0148-0227/06/2005JC003361$09.00

frequency-dependent response to the tidal forces. Models of the ocean tide potential must typically be derived a priori from global ocean tide height models. The ocean tide height models are derived from global empirical data, the application of hydrodynamic equations of motion, or a combination of these two methods. Significant improvements in the accuracy of global ocean tide height models have been achieved over the last decade. Most of these improvements can be attributed to the availability of high accuracy global sea surface height measurements from satellite altimeter missions, particularly from the TOPEX/POSEIDON (T/P) mission [*Fu et al.*, 1994]. Advances in hydrodynamic modeling have also contributed to these improvements especially when the altimetric data are used to constrain the equations of motion. The T/P-era ocean tide height models have accuracies of approximately 2–3 cm root-mean-square (RMS) or better in the deep oceans [*Shum et al.*, 1997]. Even with these advances *Ray et al.* [2003], *Knudsen* [2003], and *Knudsen and Andersen* [2002] demonstrate that commission errors in the ocean tide potential models, as reflected by the inherent accuracy of the currently available global ocean tide height models, are expected to be larger than the GRACE performance goals.

[5] The tidal spectrum is composed of hundreds of frequencies that can be derived from linear combinations of six fundamental luni-solar astronomical arguments [e.g., *Cartwright and Taylor*, 1971]. An ideal ocean tide potential model would incorporate all tidal frequencies to full spatial resolution. However, the available global ocean tide height models do not explicitly provide an independent model of the response at each tidal frequency. Instead the ocean tide height at any frequency is inferred by assuming that the unit response, or admittance, is a smooth function across the tidal spectrum. The smooth admittance assumption can be enforced either a priori to empirically determine the admittance function parameters, [e.g., *Cartwright and Ray*, 1990; *Desai and Wahr*, 1995], or after the fact on models of the ocean tide height at a few dominant tidal frequencies [e.g., *Lefèvre*, 2002; *Ray*, 1999]. Various mathematical formulations are used to model the smooth admittance function. These include the Fourier series model that is adopted by the convolution formalism of MC66, polynomial functions of frequency, and the most basic linear interpolation in frequency of the admittance at a few independently modeled frequencies. The total ocean tide height, and subsequently the respective potential, is then the sum total of the contributions from each individual frequency in the tidal spectrum.

[6] Traditional ocean tide potential models usually adopt a harmonic approach where firstly a smooth admittance assumption is used to determine the respective potential at each of a list of desired tidal frequencies, and secondly the total potential is formed from the explicit sum of the contribution from each of these frequencies. Usually these models are defined as the sum of only a subset of tidal frequencies to some maximum spherical harmonic degree and order depending on the magnitude of their individual contributions [e.g., *McCarthy and Petit*, 2004]. In some cases only those specific terms of the spherical harmonic expansion and tidal spectrum that are resonant for satellite orbit determination applications are used instead of the full spherical harmonic expansion to the defined maximum degree. Analytic perturbation analyses are often used to provide an a prior estimate of those terms that need to be included in the ocean tide potential model [e.g., *Bettadpur and Eanes*, 1994; *Casotto*, 1993; *Cheng*, 2002]. This approach becomes computationally expensive as the number of included tidal frequencies and spherical harmonic components increases. It also makes these models susceptible to errors from the omission of significant tidal frequencies and spherical harmonic components.

[7] We reduce these omission errors by adopting an approach that efficiently represents the complete tidal spectrum in the ocean tide potential model. We enforce the smooth admittance assumption directly within the ocean tide potential model itself and use the MC66 convolution formalism to represent the admittance function. In doing so, the complete spectrum of the ocean tide potential is implicitly represented without having to explicitly form the sum of the contributions from every tidal frequency. The convolution formalism's Fourier series model of the smooth admittance function in the frequency domain transforms in the time domain to a weighted sum of past, present, and future values of the TGP. In their application of the convolution formalism to local ocean tide height models MC66 computed the TGP from analytically derived luni-solar ephemerides. Similarly, we apply the convolution formalism directly to the total ocean tide potential model and compute the TGP from the more precise integrated luni-solar ephemerides that are now available [e.g., *Standish*, 1998]. Reduction of omission errors in the ocean tide potential model is then achieved firstly from the fact that all frequencies in the tidal spectrum are implicitly modeled by using luni-solar ephemerides to compute the TGP. Secondly, the gain in computational efficiency from modeling the complete tidal spectrum without an explicit summation of the contribution from each frequency then facilitates expansion of the ocean tide potential to higher spherical harmonic degree and order. In this paper we derive our application of the convolution formalism to the ocean tide potential and use GRACE data to demonstrate the improvements that can be gained.

2. Tide-Generating Potential

[8] The TGP can be directly computed from luni-solar ephemerides or indirectly from harmonic developments of this potential. This distinction as well as the fact that the TGP provides a basis for defining the admittance, or unit response, of the ocean tides is important for our application of the convolution formalism. We adopt the Cartwright-Taylor-Edden [*Cartwright and Taylor*, 1971; *Cartwright and Edden*, 1973], hereinafter referred to as CTE, convention for the TGP since it is most often used to define the ocean tide admittance. The CTE convention for the TGP, $V_T(t, \phi, \lambda)$, at some time t, latitude ϕ, and longitude λ, is expressed by the following spherical harmonic expansion.

$$\frac{V_T(t,\phi,\lambda)}{g} = \sum_{n=2}^{\infty}\sum_{m=0}^{n} M_{nm} P_{nm}(\sin\phi)\,\mathrm{Re}\left[c^{*}_{nm}(t)e^{im\lambda}\right] \qquad (1)$$

The real part and conjugate of a complex function f are denoted by Re[f] and f^*, respectively. The amplitude of the

TGP coefficients, $c_{nm}(t)$, is dependent on the normalizing factor, M_{nm}, that is applied to the unnormalized Legendre polynomial, $P_{nm}(\sin\phi)$. The CTE normalizing factor that we adopt differs from that usually applied to spherical harmonic expansions of the geopotential and is therefore explicitly defined below.

$$M_{nm} = (-1)^m \left[\frac{(2n+1)(n-m)!}{4\pi(n+m)!}\right]^{1/2} \tag{2}$$

Normalizing the tide potential by the mean gravitational acceleration, g, conveniently allows the coefficients $c_{nm}(t)$ to have units of height.

[9] The TGP coefficients, $c_{nm}(t)$, can be derived from time series of the geocentric radial distance, r_j, latitude, ϕ_j, and longitude, λ_j, of the perturbing bodies of mass M_j. The position of the perturbing bodies is accurately known from astronomical ephemerides [e.g., *Standish*, 1998]. Consideration of only the Sun (j = 1) and Moon (j = 2) as the perturbing bodies is sufficient for most tidal applications, including the ocean tides. The coefficients $c_{nm}(t)$ are evaluated at the surface of the Earth with mean equatorial radius, a, but can be scaled by $(r/a)^n$ to arbitrary geocentric radial distance, r.

$$c_{nm}(t) = a_{nm}(t) + ib_{nm}(t) \tag{3}$$

$$= \sum_{j=1}^{2} \frac{4\pi GM_j}{gr_j} \frac{(2-\delta_{m0})}{(2n+1)} \left(\frac{a}{r_j}\right)^n \times M_{nm}P_{nm}(\sin\phi_j)e^{im\lambda_j} \tag{4}$$

δ_{m0} is the Kronecker delta. We deviate from the conventional definition of the TGP by specifically excluding the permanent tide from the definition of $c_{20}(t)$. The permanent tide corresponds to the constant component of $c_{20}(t)$ with tide potential amplitude denoted here by H_0. Specifically, we define $a_{20}(t)$ as follows, so that equation (4) then only applies to all degrees (n) and orders (m) where $(n, m) \neq (2, 0)$.

$$a_{20}(t) = \sum_{j=1}^{2} \frac{4\pi GM_j}{5gr_j} \left(\frac{a}{r_j}\right)^2 M_{20}P_{20}(\sin\phi_j) - H_0 \tag{5}$$

This approach is taken to ensure that the permanent tide is excluded from our application of the convolution formalism to the ocean tide potential, since the permanent tide is usually considered to contribute to the mean sea surface rather than the ocean tide. The IERS2003 standards [*McCarthy and Petit*, 2004] recommend a permanent tide potential amplitude of $H_0 = -0.31460$ meters.

[10] Harmonic developments of the TGP, such as the CTE development, perform spectral analyses on the coefficients $c_{nm}(t)$ so that they can be represented by a series with hundreds of frequencies.

$$c_{nm}(t) = \sum_k H_{nmk} e^{-i(\omega_{nmk}t + \beta_{nmk})} \tag{6}$$

The tidal frequencies ω_{nmk} and astronomical phase angles β_{nmk} can be derived from linear combinations of the six fundamental luni-solar astronomical arguments using the Doodson argument number, $d_1d_2d_3.d_4d_5d_6$ [*Doodson*, 1921], where $d_1 = m$.

$$\omega_{nmk}t + \beta_{nmk} = d_1\tau_m + (d_2-5)s + (d_3-5)h + (d_4-5)p + (d_5-5)N' + (d_6-5)p' - \delta(n,m)\frac{\pi}{2} \tag{7}$$

$$\delta(n,m) = \begin{cases} 1 \text{ if } (n+m) \text{ odd} \\ 0 \text{ if } (n+m) \text{ even} \end{cases} \tag{8}$$

The astronomical argument τ_m represents mean lunar time, s, h, p, and p' respectively represent the mean longitude of the Moon, the Sun, the lunar perigee, and the solar perigee, and N' represents the negative mean longitude of the ascending lunar node. The angle $\delta(n, m)\,\pi/2$ ensures that the tidal phase angles conform to the CTE conventions. In practice harmonic developments of the TGP must limit the series in equation (6) and therefore provide only those tidal amplitudes, H_{nmk}, that exceed some defined threshold.

[11] There are two advantages to using equations (4) and (5) rather than equation (6) to compute the TGP. Firstly, use of the astronomical ephemerides provides the complete spectral content of $c_{nm}(t)$ without any application of threshold limits on the amplitudes H_{nmk}, and is therefore not susceptible to errors from the omission of tidal frequencies. Secondly, using the astronomical ephemerides is more efficient. For each degree and order of the TGP equations (4) and (5) involve the summation of two terms, for the Sun and Moon, while also requiring computation of the luni-solar positions from astronomical ephemerides. In contrast, similar spectral content and accuracy requires the summation of the contribution from hundreds of frequencies in equation (6) as well as the computation of the tidal phase angles, $\omega_{nmk}t + \beta_{nmk}$ for each of those terms. As such, the body tide potential is usually computed from luni-solar ephemerides rather than from harmonic developments of the TGP [e.g., *McCarthy and Petit*, 2004]. We similarly take advantage of these benefits when applying the convolution formalism to the ocean tide potential.

3. Convolution Formalism Model of the Ocean Tide Potential

3.1. The Convolution Formalism

[12] Models of the ocean tide height are typically restricted to the oceanic response to the second degree (n = 2) component of the TGP only. The ocean tide response to higher degrees is considered to be small enough to ignore for most applications and global models for these ocean tides may not exist currently. For example, equation (4) shows that the TGP coefficients are proportional to the ratio $(a/r_j)^n$. The radial distance to the Moon is approximately 60 Earth radii so the degree 3 ocean tides should be smaller than the degree 2 ocean tides by a factor of 60. As is inferred by equation (7), the spectrum of the second degree TGP is concentrated in three distinct bands. These three bands, the long-period, diurnal and semidiurnal bands, are centered at approximately m = 0, 1 and 2 cycles per day (cpd). Each band of this forcing function has its own unique spatial dependence so the unit oceanic response, namely the ocean tide admittance,

is expected to be a smooth function of frequency within each band [*Munk and Cartwright*, 1966; *Le Provost et al.*, 1991].

[13] The ocean tide height at a particular tidal frequency, $\zeta(\omega_{2mk}, \phi, \lambda, t)$, can be expressed in a similar form to the forcing function at that frequency (equation (6)) [e.g., *Cartwright and Ray*, 1990].

$$\zeta(\omega_{2mk}, \phi, \lambda, t) = H_{2mk}\mathrm{Re}\left[Z^*(\omega_{2mk}, \phi, \lambda)e^{-i(\omega_{2mk}t+\beta_{2mk})}\right] \quad (9)$$

The complex admittance, $Z(\omega_{2mk}, \phi, \lambda) = X(\omega_{2mk}, \phi, \lambda) + iY(\omega_{2mk}, \phi, \lambda)$, then defines the unit response of the ocean tide at a particular frequency, and is determined by normalizing the ocean tide height by the respective TGP forcing amplitude, H_{2mk}. It reflects the frequency dependent response of the oceans to a forcing function of particular spherical harmonic degree and order spatial distribution.

[14] The convolution formalism of MC66 uses a Fourier series of period $2\pi/\tau$ to model the smooth frequency dependent admittance function in each tidal band.

$$Z(\omega_{2mk}, \phi, \lambda) = \sum_{s=-S}^{S} U_{2m}(\phi, \lambda, s)e^{-i\omega_{2mk}s\tau} \quad (10)$$

The integer index s denotes each term of the Fourier series expansion. The complex coefficients of this Fourier series are the frequency independent convolution weights, $U_{2m}(\phi, \lambda, s) = u_{2m}(\phi, \lambda, s) + iv_{2m}(\phi, \lambda, s)$. The total ocean tide height from all frequencies in a particular tidal band can then be derived by combining equations (6), (9) and (10).

$$\begin{aligned}\zeta^{2m}(\phi, \lambda, t) &= \sum_k \zeta(\omega_{2mk}, \phi, \lambda, t) \\ &= \mathrm{Re}\left[\sum_{s=-S}^{S} U^*_{2m}(\phi, \lambda, s)c_{2m}(t - s\tau)\right]\end{aligned} \quad (11)$$

In the time domain the convolution formalism computes the total ocean tide height in each tidal band from the weighted sum of past, present and future values of the TGP coefficients in that band, $c_{2m}(t)$. Computation of the total ocean tide height, and therefore the total ocean tide potential, then also benefits from the relatively inexpensive computation of the coefficients $c_{2m}(t)$ using luni-solar ephemerides, namely using equations (4) and (5). In doing so, every tidal frequency implicitly contributes to that total. In each tidal band a summation over hundreds of frequencies can then be replaced by a summation over $(2S + 1)$ terms and $S < 3$ should be sufficient, as is described below.

[15] The orthogonalized convolution formalism of *Groves and Reynolds* [1975] is sometimes used to model the smooth admittance function, where an orthogonal basis set of functions, orthotides, are used to represent the ocean tide height. The orthotides are simple linear combinations of the Fourier series basis functions so the convolution and orthotide formulations both effectively use a Fourier series to model the smooth admittance function. The use of orthotides may provide some benefits to the empirical determination of ocean tide models from a short duration of observations, but is otherwise unnecessary. They are certainly unnecessary if the objective is only to derive the smooth admittance function from available tide height models at specific tidal frequencies. In this case the number of degrees of freedom in the admittance function model is likely to be more important than the form of the basis functions. For example, *Desai and Wahr* [1995] used T/P sea surface data to demonstrate that polynomial and orthotide, and therefore convolution, approaches to modeling the smooth admittance function provided similar results as long as they are defined by an identical number of parameters.

[16] Oceanography applications usually only require time series of the total ocean tide height at specific locations. Furthermore, the accuracy of the tide heights that is needed allows them to be computed from a subset of tidal frequencies rather than from the complete tidal spectrum. The total ocean tide height at some location can then be efficiently computed by linearly interpolating global latitude and longitude grids of the tide height models at the individual frequencies, and secondly by considering a relatively few tidal frequencies, sometimes as few as 30 diurnal and semidiurnal frequencies. In contrast, the burden of computing the contribution of each tidal frequency to the ocean tide potential escalates as the number of considered frequencies increases because the effect of the ocean tides across the globe, as represented by spherical harmonic expansions, is required. At any instant in time the total ocean tide potential should be derived from the sum of each spherical harmonic component as well as the sum of the contribution of each considered frequency. The explicit summation across the tidal spectrum can be eliminated by directly applying the convolution formalism together with TGP coefficients computed from luni-solar ephemerides to spherical harmonic decompositions of the total ocean tide height.

[17] The spatial dependence of the total ocean tide height in each tidal band is exclusively represented by the complex convolution weights (see equation (11)), so spherical harmonic decompositions of the convolution weights are determined instead of the tide height at each frequency.

$$\begin{aligned}U_{2m}(\phi, \lambda, s) = &\sum_{l=0}^{\infty}\sum_{p=0}^{l} N_{lp}P_{lp}(\sin\phi) \\ &\times \left[D^{2m}_{lp}(s)\cos p\lambda + E^{2m}_{lp}(s)\sin p\lambda\right]\end{aligned} \quad (12)$$

For consistency, when defining the complex normalized coefficients $D^{2m}_{lp}(s)$ and $E^{2m}_{lp}(s)$ we adopt the spherical harmonic normalizing factor N_{lp} that is usually adopted in definitions of the geopotential. This factor is explicitly shown below to avoid any confusion with that used by the CTE development of the TGP.

$$N_{lp} = \left[\frac{(2l+1)(l-p)!(2-\delta_{p0})}{(l+p)!}\right]^{1/2} \quad (13)$$

After combining equations (11) and (12) the total ocean tide height in each tidal band can then be similarly expressed by spherical harmonic expansions with normalized coefficients

$A_{lp}^{2m}(t)$ and $B_{lp}^{2m}(t)$ that are functions of the convolution weight coefficients.

$$\zeta^{2m}(\phi,\lambda,t) = \sum_{l=0}^{\infty}\sum_{p=0}^{l} N_{lp}P_{lp}(\sin\phi) \times \left[A_{lp}^{2m}(t)\cos p\lambda + B_{lp}^{2m}(t)\sin p\lambda\right] \quad (14)$$

$$\begin{pmatrix} A_{lp}^{2m}(t) \\ B_{lp}^{2m}(t) \end{pmatrix} = \mathrm{Re}\left[\sum_{s=-S}^{S}\begin{pmatrix} D_{lp}^{2m*}(s) \\ E_{lp}^{2m*}(s) \end{pmatrix} c_{2m}(t-s\tau)\right] \quad (15)$$

The limit of the Fourier series, S, is not required to be identical in each tidal band.

3.2. Convolution Formalism Parameters

[18] Application of the convolution formalism requires definition of the lag interval, τ, the Fourier series limit, S, and the corresponding convolution weights in each tidal band. A description of the conversion of global ocean tide height models into spherical harmonic decompositions of the convolution weights is provided in Appendix A, but requires definition of τ and S.

[19] In the long-period tidal band the ocean tides are expected to have a response that is close to equilibrium with the TGP. Any departures from equilibrium are expected to be small and to decrease with increasing period [e.g., *Desai and Wahr*, 1995]. As such, we model the long-period admittance function as a constant, namely with $S = 0$, so that τ need not be defined. We define this constant admittance function to be the self-consistent equilibrium model [e.g., *Ray and Cartwright*, 1994; *Desai and Wahr*, 1995], and use a model that was derived with methods similar to those used by *Desai* [2002] to derive the self-consistent equilibrium ocean pole tide.

[20] Choosing S in the diurnal and semidiurnal tidal bands requires two considerations. Firstly, the Fourier series of the convolution formalism provides $2S + 1$ degrees of freedom in the model of the smooth admittance function so the ocean tide response at $2S + 1$ tidal frequencies, or subbands within each tidal band, should be distinctly observable within each tidal band. Secondly, increasing S will tend to increase the number of ripples in the admittance function. So S should be large enough to accommodate sufficiently separate normal modes of the oceanic response within each tidal band, but should not be so large that it introduces unrealistic ripples in the admittance function. Using tide gauge observations MC66 and *Zetler and Munk* [1975] concluded that $1 \leq S \leq 3$ is an appropriate range for the diurnal and semidiurnal bands. *Desai and Wahr* [1995] concluded that $S = 1$ was optimal for empirical global models of the diurnal and semidiurnal ocean tides that were determined from less than three years of T/P sea surface height observations. With more than a decade of T/P data now available that analysis could be revisited to determine any benefits from increasing S. However, $S > 2$ is not likely to provide any significant benefit, and is likely to add too many ripples into the smooth admittance model.

[21] We derive the convolution weights from available ocean tide height models so the $2S + 1$ degrees of freedom proves to be our limiting constraint. Derivation of the convolution weights requires models of the ocean tide height for at least $2S + 1$ distinct tidal frequencies, and the ocean tides at each of these frequencies should be expected to conform to the smooth admittance assumption. The smooth admittance function that is defined by these convolution weights then provides a first order estimate of the response at every tidal frequency in the particular tidal band that it represents. Any deviations from the smooth function can then be modeled as corrections to the convolution model, as is described in section 3.3.

[22] In practice corrections to the convolution model are only necessary at a few frequencies. The S1, S2, and K1 ocean tides, at least, are expected to have significant departures from the smooth admittance assumption and ideally they should not be used to derive the convolution weights. Observations of the oceanic response at the S1 and S2 frequencies are composed of the sum total of the gravitational and radiation ocean tides. The gravitational ocean tide is the response to the luni-solar tidal potential which should comply with the smooth admittance assumption. The radiation ocean tide refers to the additional response to non-gravitational effects such as atmospheric forcing [e.g., *Ray and Egbert*, 2004] which is largest at these two tidal frequencies. The free core nutation (FCN) resonance causes deviations from the smooth admittance function in diurnal tides that have frequencies close to the FCN normal mode frequency of approximately 1.00492 cpd [*Desai and Wahr*, 1995; *Wahr and Sasao*, 1981]. This resonance is expected to amplify the admittance of the largest diurnal tide, the K1 tide, by 6%. Most of the other diurnal tides that are affected by the FCN resonance have relatively small TGP amplitudes so that the effect on their respective tide heights is likely to be small enough to ignore for most applications. For example, the FCN resonance is expected to attenuate the $\psi 1$ and $\phi 1$ ocean tide admittances by 24 and 4%, respectively, but their TGP amplitudes are more than a factor of 70 smaller than that of the K1 tide.

[23] Even the best available ocean tide height models at this time typically only independently derive the response at four or five frequencies in each of the diurnal and semidiurnal tidal bands. The response at other frequencies is then inferred from smooth admittance assumptions. For example, the GOT00.2 model, a recent version of the empirical model by *Ray* [1999], explicitly provides global maps of 3 diurnal (Q1, O1, and K1) and 4 semidiurnal (N2, M2, S2, and K2) frequencies. Similarly, the FES2004 model, a recent version of the empirically constrained hydrodynamic model of *Lefèvre* [2002], explicitly provides global maps for 4 diurnal (Q1, O1, P1, and K1) and 5 semidiurnal (2N2, N2, M2, S2, and K2) frequencies. The software packages provided with each tide height model then apply smooth admittance assumptions to infer the response at other frequencies. After excluding the S2 ocean tide, for reasons described above, both models can then only accommodate $S = 1$ in the convolution formalism for each of the diurnal and semidiurnal tidal bands. Our results are limited to these two ocean tide models so we always use $S = 1$ in the diurnal and semidiurnal tidal bands.

[24] The bandwidth, ΔF, of the tidal band that is being modeled by the smooth admittance function provides an estimate of the lag interval, τ. As stated by MC66, choosing

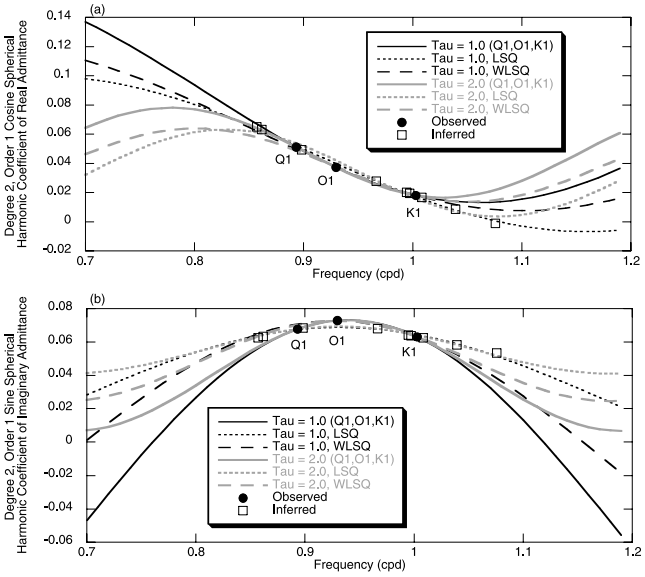

Figure 1. Comparison of admittance functions for the degree 2 order 1 spherical harmonic component of the diurnal tidal band as derived from the GOT00.2 ocean tide model. The solid circles and squares, respectively, show the admittance for the three observed (Q1, O1, K1) and nine inferred tidal components that are provided by the model. Black and grey lines respectively show convolution admittance functions that are derived with $\tau = 1.0$ and 2.0 days. Solid, dotted, and dashed lines respectively represent convolution functions where the convolution weights are derived from an exact fit to the three observed tidal components, an equally weighted least squares fit (LSQ) to all observed and inferred tidal components, and a weighted least squares fit (WLSQ) to all observed and inferred tidal components.

$1/\tau > 2\Delta F$ improves convergence of the Fourier series and limits errors at the outer edges of the modeled tidal band. The CTE harmonic development of the TGP defines the diurnal and semidiurnal tidal bands with bandwidths of 0.3 cpd each, ranging from 0.8–1.1 and 1.8–2.1 cpd, respectively. In contrast, the more recent development by *Tamura* [1987] defines bandwidths of 0.5 cpd, ranging from 0.7–1.2 and 1.7–2.2 cpd, respectively. However, the largest tidal components in these two bands are concentrated in the middle of each band, while the outer edges consist of much smaller tidal components that may not be detectable, depending on the application. So although the CTE and *Tamura* [1987] developments respectively infer $\tau < 1.7$ and 1.0 days the use of lengthier lag intervals implies that the contribution from the outer edges of the tidal bands are considered to be negligible. MC66 adopted $\tau = 2$ days based on some tests with tide gauge data.

[25] The impact of two lag intervals, $\tau = 1$ and 2 days, on the dominant spherical harmonic components of the diurnal and semidiurnal admittance functions is illustrated in Figures 1 and 2, using the GOT00.2 ocean tide model. These figures also show the effect of three different approaches to deriving the convolution weights. The weighted least squares approach weights each of the observed and inferred tidal components by H^2_{nmk} during the least squares estimation of the convolution weights and the resulting convolution weights should most closely resemble those that would result from their empirical determination from a time series of the total ocean tide. From both figures it is apparent that linear interpolation and extrapolation of the observed tidal components was used to derive the inferred GOT00.2 tidal components that were provided to us (R. Ray, personal communication, 2005). Adjustment of the K1 admittance for the free core nutation resonance was not applied to the diurnal admittances shown in Figure 1 to better illustrate the admittance relationships that were adopted by the GOT00.2 model.

[26] The various admittance functions are similar at the central frequencies, between the independently observed tidal components. Meanwhile significant differences exist at the outer edges of the tidal bands where each model essentially provides a different extrapolation of the admittance function. Without independent validation there is no reason to assume that any one of the approaches is superior, including the linear extrapolation adopted by the GOT00.2 model. However, the different extrapolations are only important if the outer edges of the tidal bands contain tidal components that are large enough to have an impact on the application at hand.

[27] The shorter lag interval of 1-day generally provides an admittance function that most closely resembles a linear extrapolation at the outer edges of the tidal bands. As expected, the longer 2-day lag interval introduces significant sinusoidal variations to the admittance function at the outer edges of the tidal bands. The equally weighted least squares approach with $\tau = 1$ day fits the GOT00.2 linearly extrapolated admittances best of all the methods. The disadvantage of the two least squares approaches is that neither exactly fits any of the observed or inferred admit-

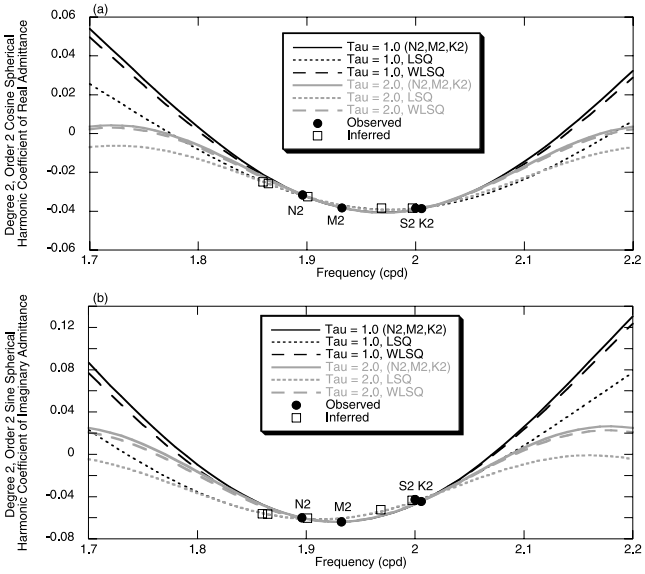

Figure 2. Same as Figure 1, except for the degree 2 order 2 spherical harmonic component of the semidiurnal tidal band as derived from the GOT00.2 ocean tide model. The four observed tidal components are N2, M2, S2, and K2, there are five inferred components, and S2 is excluded from all derivations of the convolution weights.

tances from the model. Application of the convolution formalism may therefore require small corrections at least for the observed tidal components to account for differences with respect to the convolution function. This adds to the computational overhead of computing the ocean tide potential. In contrast, exactly fitting the three observed tidal components has the computational advantage that no corrections to the convolution model are required for the three observed tidal components in each band.

3.3. Corrections to the Convolution Model

[28] As described earlier, small corrections to the convolution model may be necessary for the few tidal components that are expected to have significant departures from the smooth admittance assumption, for example for the S1, S2, and K1 tidal components as discussed earlier. Similarly, exact representation of other tidal components that have explicitly defined tide height models can also be ensured by applying corrections to the convolution model. For example, some long-period ocean tides are provided by the FES2004 model and can be exactly represented using corrections to the constant admittance model that is assumed in the long-period band.

[29] Corrections to the convolution model of the ocean tide potential to account for deviations from the smooth admittance function are easily determined from spherical harmonic decompositions of these deviations, $\Delta Z(\omega_{2mk}, \phi, \lambda)$.

$$\Delta Z(\omega_{2mk}, \phi, \lambda) = Z(\omega_{2mk}, \phi, \lambda) - \bar{Z}(\omega_{2mk}, \phi, \lambda) \tag{16}$$

$$= \sum_{l=0}^{\infty} \sum_{p=0}^{l} N_{lp} P_{lp}(\sin\phi) \times \left[\Delta A^{Z}_{lp}(\omega_{2mk}) \cos p\lambda + \Delta B^{Z}_{lp}(\omega_{2mk}) \sin p\lambda \right] \tag{17}$$

$Z(\omega_{2mk}, \phi, \lambda)$ is the admittance derived from the provided tide height model, and $\bar{Z}(\omega_{2mk}, \phi, \lambda)$ is the admittance at that frequency as computed by the convolution model. From equation (9) these departures from the smooth admittance model translate into the following corrections to the total ocean tide height spherical harmonic coefficients.

$$\begin{pmatrix} \Delta A^{2m}_{lp}(\omega_{2mk}, t) \\ \Delta B^{2m}_{lp}(\omega_{2mk}, t) \end{pmatrix} = H_{2mk} \mathrm{Re} \left[\begin{pmatrix} \Delta A^{Z*}_{lp}(\omega_{2mk}) \\ \Delta B^{Z*}_{lp}(\omega_{2mk}) \end{pmatrix} e^{-i(\omega_{2mk} t + \beta_{2mk})} \right] \tag{18}$$

In this way corrections to the convolution model can be applied, as desired, at any tidal frequency that has appreciable departures from the smooth admittance model.

3.4. Ocean Tide Potential

[30] The geopotential, $\Delta V(r, \phi, \lambda)$, is usually expressed by a spherical harmonic expansion with normalized coefficients $\Delta C_{lp}(t)$ and $\Delta S_{lp}(t)$,

$$\Delta V(r, \phi, \lambda) = \frac{GM}{r} \sum_{l=1}^{\infty} \sum_{p=0}^{l} \left(\frac{a}{r}\right)^{l} N_{lp} P_{lp}(\sin\phi) \times \left[\Delta C_{lp}(t) \cos p\lambda + \Delta S_{lp}(t) \sin p\lambda \right] \tag{19}$$

The contribution of the ocean tides to temporal variations of these geopotential coefficients is then the sum total of the convolution model of the total ocean tide height in each band and the corrections at each tidal frequency that is expected to have significant deviations from the convolution model.

$$\begin{pmatrix} \Delta C_{lp}(t) \\ \Delta S_{lp}(t) \end{pmatrix} = \frac{4\pi G \rho_w}{g} \frac{(1 + k'_l)}{2l + 1} \times \left[\sum_{m=0}^{2} \begin{pmatrix} A^{2m}_{lp}(t) \\ B^{2m}_{lp}(t) \end{pmatrix} + \sum_{i}^{I} \begin{pmatrix} \Delta A^{2m}_{lp}(\omega_{2mk}, t) \\ \Delta B^{2m}_{lp}(\omega_{2mk}, t) \end{pmatrix} \right] \tag{20}$$

The contribution from the deformation of the solid Earth that is caused by the load of the ocean tides, namely the load tide, is taken into account by the factor $(1 + k'_l)$, where k'_l is the degree l load Love number. The mean density of the oceans is defined by ρ_w. Equation (20) assumes the relationship $g = GM/a^2$. The summation in m explicitly shows the contribution from the total ocean tide in each of the three tidal bands, and the summation in i accounts for the small correction at each of the I frequencies with significant departures from the smooth admittance model.

4. Application to GRACE

4.1. Contributions to Geoid Height

[31] Use of the smooth admittance assumption provides the opportunity to determine a first order estimate of the contribution of each tidal frequency to variations of geoid height. The total admittance at any tidal frequency $Z(\omega_{2mk}, \phi, \lambda)$ can be decomposed into its spherical harmonic components using a similar form to the admittance differences shown in equation (17), but using total admittance coefficients $A^{Z}_{lp}(\omega_{2mk})$ and $B^{Z}_{lp}(\omega_{2mk})$ instead of the difference coefficients $\Delta A^{Z}_{lp}(\omega_{2mk})$ and $\Delta B^{Z}_{lp}(\omega_{2mk})$, respectively. Following *Wahr et al.* [1998] and *Ray et al.* [2003] the degree amplitude spectrum of the variations in the geoid caused by that ocean tide component, $\delta N_l(\omega_{2mk})$, is derived from the RMS over one tidal period.

$$\delta N_l(\omega_{2mk}) = \frac{3\rho_w}{\rho_e} \frac{(1 + k'_l)}{2l + 1} \times \left[\frac{H^2_{2mk}}{2} \sum_{p=0}^{l} \left(|A^{Z}_{lp}(\omega_{2mk})|^2 + |B^{Z}_{lp}(\omega_{2mk})|^2 \right) \right]^{1/2} \tag{21}$$

The mean density of the Earth is denoted by ρ_e.

[32] The contribution to geoid height from the total ocean tide in each band is shown in Figure 3 and is computed from the root-sum-square of the contribution from each frequency in that band. The admittance of each tidal component is derived from the self-consistent equilibrium model of the long-period tides, and a convolution formalism model with $\tau = 1$ day applied to the GOT00.2 model of the diurnal and semidiurnal ocean tides. The results shown do no change significantly when $\tau = 2$ days is used instead, especially at the scales shown. The tide potential amplitudes, H_{2mk}, are taken from the harmonic development of *Tamura* [1987]

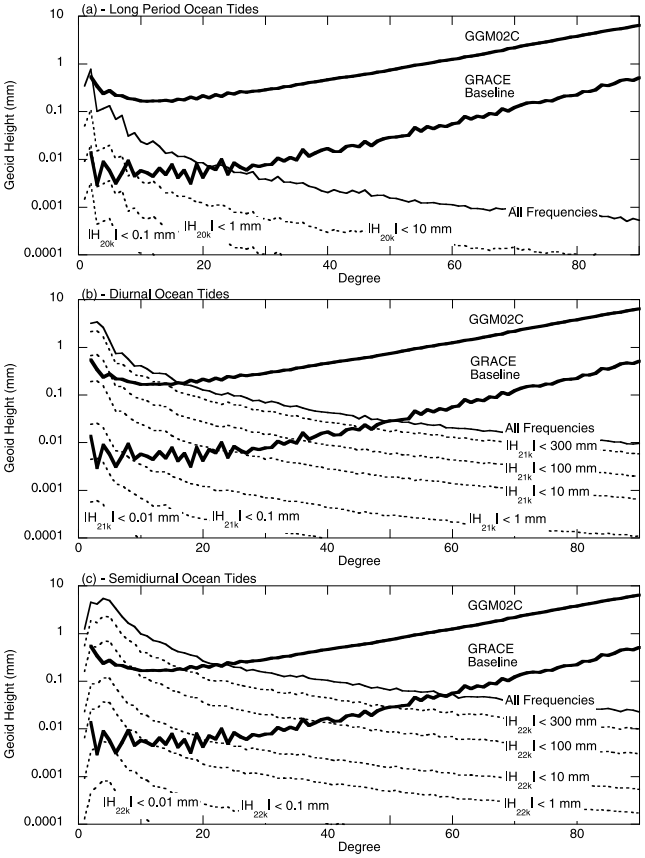

Figure 3. Degree variance of the contribution of the (a) long-period, (b) diurnal, and (c) semidiurnal ocean tides to the geoid height. The two thick solid lines show the prelaunch baseline performance goal for the GRACE mission, and the formal errors in the GGM02C GRACE gravity field. The solid line shows the contribution from all spectral components in each band, while the dashed lines show the contribution of only those tidal frequencies that satisfy the indicated threshold limits on the magnitude of the respective tide potential amplitude, $|H_{nmk}|$.

since it provides a more comprehensive representation of the tidal spectrum than the CTE development. For comparison the baseline performance goals for GRACE and the formal errors in the currently best available GRACE-derived gravity field, GGM02C, are also shown (S. Bettadpur, personal communication, 2005).

[33] In an effort to determine the tidal components that are significant to achieving the GRACE performance goals, Figure 3 also shows the contribution from subsets of tidal components in each band as derived by applying thresholds to the tide potential amplitudes H_{2mk}. The only components with $|H_{2mk}| \geq 300$ mm are the M2 and K1 components and should be taken to at least spherical harmonic degree 60 and 50, respectively, to achieve the GRACE performance goals. Similarly, the O1, P1, N2, and S2 components, as the additional components with $|H_{2mk}| \geq 100$ mm, should be taken to at least degree 45. Considering those tidal components with $|H_{2mk}| \geq 10$ mm then in total 6 long-period components should be taken to at least degree 20, 9 diurnal components to at least degree 35, and 11 semidiurnal component to at least degree 40. These include the 18.6 year, Ssa, Mm, Mf, Mt, Q1, M1, J1, OO1, 2N2, μ2, ν2, L2, T2, and K2 components, as well as the nodal modulations of the Mf, O1, K1, M2 and K2 tidal components. The diurnal and semidiurnal components with $|H_{2mk}| \geq 0.1$ mm and long period components with $|H_{2mk}| \geq 1$ mm should be considered to degree 10. In total this consists of 114 diurnal, 85 semidiurnal, and 20 long period components. The tidal components of smaller amplitude are not likely to have a significant impact on the GRACE performance goals. A convolution model with $S = 1$ requires 3 complex coefficients in each band and therefore has similar computational burden to individually modeling the six diurnal and semidiurnal components that need to be modeled to at least degree 45. However, the convolution model will then also implicitly model to high degree all of the almost 200 diurnal and semidiurnal components that should be modeled at the low degrees.

[34] An alternative approach, and one that is of significance to the smooth admittance model, is to separate the ocean tide contributions to geoid height by tidal group number, as shown in Figure 4. The first two digits of the Doodson number, d_1d_2, define the tidal group number where $d_1 = 0$, 1 and 2 for the long-period, diurnal, and semidiurnal tidal bands, respectively. For convenience we define $g_2 = d_2 - 5$ so that each tidal group consists of clusters of tidal frequencies that are centered around $0.96614\ d_1 + 0.03660\ g_2$ cpd. Each tidal band is then centered at the tidal group with $g_2 = 0$, and g_2 increasingly deviates from zero towards the outer regions of the tidal band. The CTE harmonic development defines the degree 2 TGP for groups with $|g_2| \leq 4$, while the *Tamura* [1987] development defines it for $|g_2| \leq 7$. This explains the

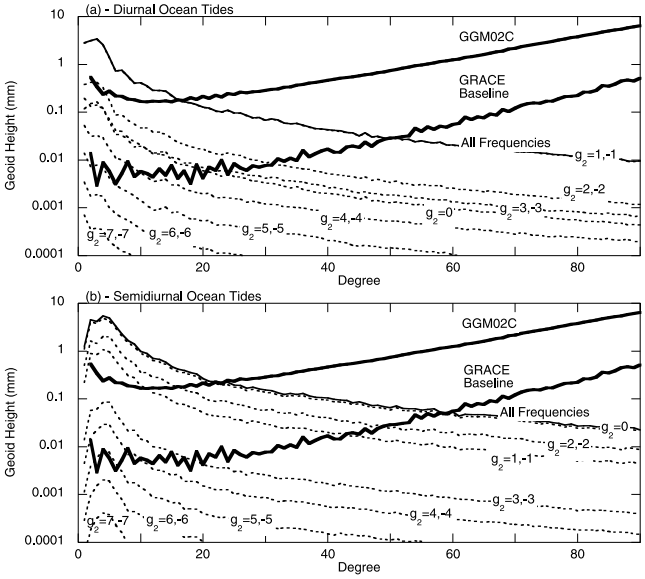

Figure 4. Same as Figure 3, but only for the (a) diurnal and (b) semidiurnal ocean tides, and with the dashed lines showing the contribution of all tidal frequencies in each tidal group. Tidal group number is taken from the first two digits of the Doodson argument number, d_1d_2, where $d_1 = 1$ in the diurnal band and $d_1 = 2$ in the semidiurnal band. Group number is denoted in the figure by using $g_2 = d_2 - 5$.

0.2 cpd wider bandwidth available from the *Tamura* [1987] development.

[35] The largest amplitude diurnal and semidiurnal tidal components occur at the central groups where $|g_2| \leq 2$. The dominant tidal components in these groups are explicitly provided by the tide height models and provide an important constraint to the diurnal and semidiurnal convolution functions in this region of the tidal spectrum. As illustrated in Figures 1 and 2, the uncertainty of the admittance function is therefore expected to be smallest for the ocean tides in these central groups where $|g_2| \leq 2$. However, at the outer groups where $|g_2| > 2$ the admittance function is effectively defined by an extrapolation since no constraint is available from the tide height models. The uncertainty of this extrapolation is expected to gradually increase towards the outer tidal groups. Fortunately, the amplitude of the tidal components decreases towards the outer tidal groups and consequently reduces the impact of the increasing admittance function uncertainties on the ocean tide potential models. For example, Figure 4 shows that the contributions to geoid height from the extreme outer groups where $|g_2| = 6$ and 7 are below the GRACE performance goals so the large uncertainty in the admittance function at these frequencies is not expected to have an impact on these goals. The mid-groups where $|g_2| = 3$ and 4 need to be taken to approximately degrees 20 and 10, respectively, but the uncertainty of the admittance function extrapolation is expected to be smallest at these groups. The contribution of the ocean tides from groups with $|g_2| = 5$ in the diurnal and semidiurnal bands lies at the GRACE performance goals at degrees less than 10 and may have an impact on GRACE performance. Inclusion of the tides in this group through the application of a smooth admittance approach with harmonic developments of the TGP would then require more extensive developments than is available from CTE, such as that from *Tamura* [1987]. In contrast, use of a TGP derived from luni-solar ephemerides inherently includes all groups.

[36] The sensitivity of GRACE to the diurnal and semidiurnal groups where $|g_2| \leq 4$ reduces the effective bandwidth of the diurnal and semidiurnal bands to approximately 0.29 cpd, so that longer lag intervals of less than 2.3 days can be used for the GRACE ocean tide potential convolution models. The non-negligible contributions of the diurnal and semidiurnal ocean tides with groups $|g_2| = 3$ an 4 also suggests potential for improvement of the GRACE ocean tide potential convolution models. Specifically, the extrapolation of the admittance functions at these groups could be eliminated by extending the Fourier series of the diurnal and semidiurnal convolution models to $S = 2$ at least up to degree 20 using tide height models at two frequencies in these groups.

4.2. Results From GRACE

[37] The GRACE mission consists of a pair of satellites that have an inter-satellite dual frequency one-way K-band ranging system. The GRACE gravity fields are determined from a least squares fit to the difference between the K-band range rate (KBRR) measurements and the respective range rate that is computed from a nominal orbit for the pair of satellites [*Tapley et al.*, 2004b]. The nominal orbit is computed by using a priori models of the static and temporally varying gravity field, and measurements from an accelerometer and global positioning system receiver on each satellite. The KBRR observations effectively provide a measure of the observed gravity field so we use the postfit KBRR residuals, namely the residuals after estimating the monthly GRACE gravity fields, to evaluate the impact of the various ocean tide potential models.

[38] We use the Mirage software package from the Jet Propulsion Laboratory to process the GRACE data. Daily nominal orbit solutions are first generated and then combined to estimate monthly gravity fields to degree 120. In all cases the nominal orbit uses the GRACE-derived GGM01C static gravity field [e.g., *Tapley et al.*, 2004a, 2004b], the IERS2003 conventions for the solid Earth tide model [*McCarthy and Petit*, 2004], and identical models for the contributions to the geopotential from the atmosphere and non-tidal ocean circulation. Two monthly gravity solutions, September and October of 2003, are used to evaluate the various ocean tide potential models. Six days during the September 1 to October 31 evaluation period are excluded from the monthly gravity solutions because of known problems with the GRACE data on those days.

[39] Initial tests are performed to determine the sensitivity of the ocean tide potential convolution model, as derived from the GOT00.2 tide height model, to the lag interval and the method used to derive the diurnal and semidiurnal convolution weights. In these studies the model for the long-period tides is fixed and the ocean tide potential is always taken to spherical harmonic degree 60. First, the use of three different lags intervals, 1, 1.5, and 2 days, to define the diurnal and semidiurnal convolution models are tested and are always applied identically to both bands. Second, three different methods are used to derive the convolution weights with each of the three lag intervals. They consist of an exact fit to the Q1, O1, and K1 tides for the diurnal weights and the N2, M2 and K2 tides for the semidiurnal weights; an equally weighted least squares fit to these six observed tidal components and the 9 diurnal and 5 semidiurnal tidal components that are inferred by linear interpolation and extrapolation of the respective observed admittances; and a weighted least squares fit to the same observed and inferred tidal components where each tidal component is weighted by the square of the respective tide potential amplitude. Corrections to the convolution model from the two least squares methods are also applied to ensure that the Q1, O1, K1, N2, M2, and K2 tidal components are modeled exactly as provided by the GOT00.2 model in all three methods.

[40] The net effect of the various lag intervals and methods for deriving the convolution weights is less than 1.5% in the postfit KBRR residual variances, as shown in Table 1. The weighted least squares method, which should most closely reflect the convolution weights that would be determined from a time series of ocean tide observations, consistently results with the largest KBRR residual variance by 0.3–1.3%. In contrast, the two other methods effectively weight the admittance at each considered tidal frequency equally and perform similarly to each other. Within each fitting method the KBRR residual variance changes by less than 0.5% for the 1–2 day range of lag intervals, so the sensitivity to lag interval is smaller than it is to the method used to fit the convolution weights. This supports the

Table 1. Postfit K-Band Range Rate Residual Variance From Two Monthly GRACE Gravity Solutions After Using Various Lag Intervals and Approaches to Derive the Diurnal and Semidiurnal Convolution Weights From the GOT00.2 Ocean Tide Model

Approach[a]	Lag Interval, τ, days	KBRR Residual Variance, $\mu m^2/s^2$	
		September	October
Exact Fit to Observed	1.0	0.04626	0.05114
Exact Fit to Observed	1.5	0.04607	0.05108
Exact Fit to Observed	2.0	0.04616	0.05108
Equally Weighted Least Squares	1.0	0.04609	0.05083
Equally Weighted Least Squares	1.5	0.04608	0.05083
Equally Weighted Least Squares	2.0	0.04611	0.05093
Weighted Least Squares	1.0	0.04641	0.05137
Weighted Least Squares	1.5	0.04639	0.05148
Weighted Least Squares	2.0	0.04632	0.05122

[a]The exact fit approach is where the convolution weights are derived from an exact fit to the observed three diurnal (Q1, O1, and K1) and three semidiurnal (N2, M2, and K2) tides. The equally weighted and weighted least squares approaches are where the convolution weights are respectively derived from a least squares fit to all of the available observed and inferred diurnal and semidiurnal tidal components. The weighted approach weights each tidal component by the square of its tide potential amplitude.

predicted small sensitivity of GRACE to the outer groups of the diurnal and semidiurnal tidal bands where changes to the lag interval and the method used to determine the convolution weights will cause the largest differences in the smooth admittance function. Nevertheless, the lag intervals of 1.5 and 2 days provide the smallest residual variances when using the exact fit approach, and have no significant impact when using the equally weighted least squares approach.

[41] Based on these results further testing of the convolution models is restricted to those that derive the diurnal and semidiurnal convolution weights from the exact fit method with a lag interval of 2 days. The exact fit convolution model exactly represents the three primary tidal components in each band. It therefore has a lower computational burden than either of the least squares methods because six fewer correction terms are required at each spherical harmonic degree and order. The relative performance of the three ocean tide potential models that are described in Table 2 are also evaluated using the monthly postfit KBRR residual variances, as illustrated in Figure 5. The overall trend of the results from each month is similar except that the residual variance from October is respectively 10% larger than in September. The ocean tides are predominantly of much shorter period than a month so we evaluate the impact of the ocean tide potential models at shorter periods by partitioning the monthly postfit KBRR residual variances by day, as shown in Figure 6. For clarity, this figure shows the daily residual variance from only the degree 60 versions of the three models described in Table 2 as a percentage of the respective residual variance from the degree 30 GOT00.2 harmonic model.

[42] One of three ocean tide potential models that are evaluated applies the traditional harmonic approach to model the ocean tide potential. In our application of the GOT00.2 harmonic model the total ocean tide potential at each spherical harmonic degree and order is formed from the sum of 12 diurnal, 9 semidiurnal, and 7 long-period tidal frequencies. In contrast, the respective GOT00.2 convolution model is formed from the sum of 4 diurnal, 4 semidiurnal, and 5 long-period complex terms at each degree and order. Although the convolution model is formed from fewer terms it does require some additional computational overhead to interpolate the luni-solar ephemerides and to compute the TGP at the three required times of $t - 2$ days, t, and $t + 2$days.

[43] The convolution model uses half the number of terms at each degree and order but results with a 4–5% smaller monthly residual variance than the harmonic model from both the degree 30 and 60 respective models. Although not explicitly shown, the daily fluctuations in Figure 6 as well as the overall variance reduction from the two convolution models result primarily from the degree 30 and lower spherical harmonic components. The degree 31 and higher spherical harmonic components reduce the daily residual variance by 1–4%. The daily postfit residual variance from the convolution model is smaller than from the harmonic model by as much as 15%, although there are two days where the residual variance is larger than from the degree 30 GOT00.2 harmonic model, but by less than 1.5%. As expected, GRACE appears to be insensitive to the degree

Table 2. Description of the Formulation of the Three Ocean Tide Potential Models Tested With GRACE Data

Model	Diurnal Band	Semidiurnal Band	Long-Period Band
GOT00.2 Harmonic	Observed: Q1, O1, K1 Inferred: 2Q1, J1, M1, OO1 ρ1, σ1, P1, ϕ1, π1	Observed: N2, M2, K2, S2 Inferred: 2N2, L2, μ2, ν2, T2	Mm, Mf, Mt, and Mq from FES2004. Sa, Ssa, and 18.6 year from self-consistent equilibrium.
GOT00.2 Convolution	Convolution weights from exact fit to Q1, O1, and P1, with τ = 2 days. Correction for observed K1.	Convolution weights from exact fit to N2, M2, and K2, with τ = 2 days. Correction for observed S2.	Constant admittance convolution weight from self-consistent equilibrium. Correction for Mm, Mf, Mt, and Mf node from FES2004[a].
FES2004 Convolution	Convolution weights from exact fit to Q1, O1, P1, with τ = 2 days. Correction for observed K1.	Convolution weights from exact fit to N2, M2, and K2 with τ = 2 days. Correction for observed S2.	Constant admittance convolution weight from self-consistent equilibrium. Correction for Mm, Mf, Mt, and Mf node from FES2004[a].

[a]The correction for the Mf nodal modulation is derived by assuming a constant admittance with the Mf tide from FES2004.

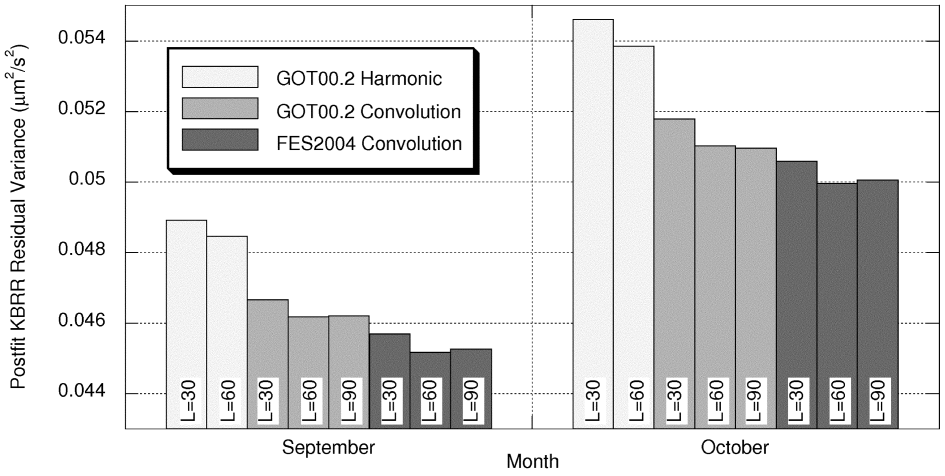

Figure 5. Postfit K-band range rate (KBRR) residual variance from monthly GRACE gravity recovery solutions in September and October 2003. The three models shown are described in Table 2. The models are taken to maximum spherical harmonic degree, L = 30, 60 and 90.

61 and higher spherical harmonic components of the ocean tides since there is no noticeable impact on the KBRR residuals from these components.

[44] An approach that is sometimes used to improve the harmonic model with minimal additional computational overhead is to apply the so-called 18.6 year nodal modulation corrections to each of the primary tidal components. These corrections take the form of time-dependent adjustments to the amplitude and phase of the primary tidal components that are derived by assuming a constant admittance between the primary component and the neighboring 18.6 year modulations. Nodal modulation corrections are applied within the ocean tide height prediction software that is provided with the GOT00.2 and FES2004 tide models, and have been implemented in the ocean tide potential model that is used in the GEODYN software package at the Goddard Space Flight Center (R. Ray, personal communication, 2005). The results from the convolution model certainly indicate that the use of nodal corrections will reduce the postfit KBRR residual variance from the harmonic model, but we have no results to suggest that the convolution approach is superior. We did not apply nodal modulation corrections in our application of the GOT00.2 harmonic model because our software did not have the existing infrastructure to do so, while our application of the convolution model inherently accounts for these modulations, and indeed models the full tidal spectrum with fewer terms than the tested harmonic model.

[45] A comparison between ocean tide potential convolution models derived from the GOT00.2 and FES2004 tide height models shows that the monthly residual variance from the degree 30 and 60 FES2004 models is 2–3% lower than that from the respective GOT00.2 models. The degree 60 FES2004 model results with a smaller residual variance

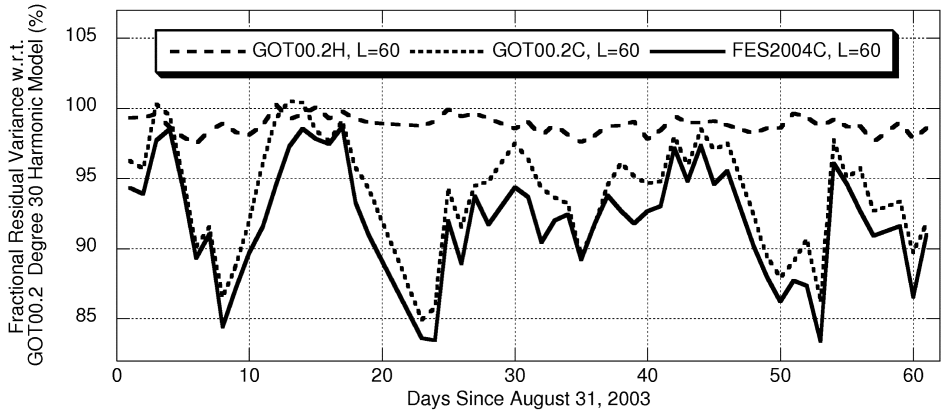

Figure 6. Daily postfit K-band range rate (KBRR) residual variance from the degree L = 60 GOT00.2 harmonic (GOT00.2H) (dashed line), GOT00.2 convolution (GOT00.2C) (dotted line), and FES2004 convolution (FES2004C) (solid line) models as a fraction of the respective postfit residual variance from the degree 30 GOT00.2 harmonic model.

than the respective GOT00.2 model on all except one of the days in the two month test period. In addition, the degree 30 FES2004 convolution model also has a smaller monthly residual variance than the degree 60 GOT00.2 model and a smaller daily residual variance on all except 12 days in the two month period. This suggests that the long wavelength components of the ocean tides are better modeled by FES2004 and is surprising because typical tide height modeling strategies that are often adopted by empirical models, such as GOT00.2, rely on hydrodynamic models to model the short wavelength variability, and then use empirical data from satellite altimetry to determine long wavelength corrections to the hydrodynamic models. The GOT00.2 model is derived from empirical corrections to a much earlier version of the FES2004 model, namely the FES94.1 model, as well as other local hydrodynamic models. Geographical maps of the postfit KBRR residuals may provide additional insight into the cause of the differing results from the two presented convolution models.

5. Conclusions

[46] Application of the convolution formalism of MC66 together with the computation of the TGP from luni-solar ephemerides provides a computationally efficient model of the complete spectrum of the ocean tide potential. The improvements to the ocean tide potential model from representing the entire tidal spectrum as well as the efficiency of the approach are demonstrated by smaller GRACE intersatellite range rate residuals from the use of the convolution model than from a more traditional harmonic model with twice the number of parameters. The monthly GRACE KBRR residual variance is smaller by 4–5% and the daily residual variance is smaller by as much as 15%.

[47] Results from the two months of GRACE data used to evaluate the ocean tide potential models appear to be sufficiently consistent to provide a reliable evaluation of the relative impact of the convolution versus harmonic approaches to modeling the ocean tide potential, and for cross comparison of the GOT00.2 and FES2004 convolution models. However, longer evaluation periods may be useful for tuning of the lag interval and method to derive the convolution weights. Further reduction of the monthly KBRR residual variance by approximately 1% may be possible by better constraining the convolution admittance function at tidal frequencies in the outer regions of the diurnal and semidiurnal tidal bands where the uncertainties in the presented function are largest. Ideally this constraint could be provided by explicit tide height models for at least two frequencies in those regions of the tidal bands, for example 2Q1 and $\eta 1$ in the diurnal band and $\epsilon 2$ and $\eta 2$ in the semidiurnal band. In doing so it may be possible to add two more terms to the Fourier series model of the diurnal and semidiurnal admittance functions and perhaps to adopt a shorter lag interval than the 2 days used here.

[48] The adopted approach of using a combination of the convolution model with corrections at discrete frequencies allows the complete spectrum of the ocean tide potential to be modeled to first order by enforcing a smooth admittance assumption across the tidal spectrum, and the few tidal frequencies at which explicit tide height models are available to be modeled exactly as provided. This approach also provides some flexibility for reducing commission errors in the ocean tide potential models through the use of GRACE data or the precise orbit determination of other Earth orbiters. One approach would be to determine corrections to the a priori convolution weights. However, this approach will provide weights that are biased towards providing the best fit to the largest tidal components rather than providing the best fitting admittance function across the tidal spectrum. An alternative approach would be the determination of corrections at a few dominant tidal frequencies and spherical harmonic components where use of a background convolution model should reduce any cross contamination or aliasing from other frequencies in the tidal spectrum.

Appendix A: Deriving the Convolution Weight Spherical Harmonic Coefficients

[49] The convolution weights for a tidal band are derived from a model of the ocean tide height at K frequencies in that band. Ideally, these K tidal components should have been derived independently without any smooth admittance assumptions relating them to each other. For reasons shown below K should be odd-valued. Global ocean tide models usually define the ocean tide height $\zeta(\omega_{2mk}, \phi, \lambda, t)$ at a particular frequency by the amplitude and Greenwich phase lag, $A(\omega_{2mk}, \phi, \lambda)$ and $G(\omega_{2mk}, \phi, \lambda)$, respectively.

$$\zeta(\omega_{2mk}, \phi, \lambda, t) = A(\omega_{2mk}, \phi, \lambda) \times \cos(\omega_{2mk} t + \beta_{2mk} - G(\omega_{2mk}, \phi, \lambda) + \delta_{2mk}\pi) \tag{A1}$$

$$\delta_{2mk} = \begin{cases} 1 \text{ when } (-1)^{\delta_{0m}} M_{2m} H_{2mk} < 0 \\ 0 \text{ when } (-1)^{\delta_{0m}} M_{2m} H_{2mk} > 0 \end{cases} \tag{A2}$$

The convolution weights for each tidal band are then derived from the following steps.

[50] Step 1: For each of the $k = 1, K$ available ocean tide height components compute maps of the in-phase and quadrature components, $\zeta^i(\omega_{2mk}, \phi, \lambda)$ and $\zeta^o(\omega_{2mk}, \phi, \lambda)$, from maps of the amplitudes and Greenwich phase lags as follows.

$$\zeta^i(\omega_{2mk}, \phi, \lambda) + i\zeta^o(\omega_{2mk}, \phi, \lambda) = A(\omega_{2mk}, \phi, \lambda) e^{iG(\omega_{2mk}, \phi, \lambda)} \tag{A3}$$

[51] Step 2: For each of the K tidal components, compute maps of the complex admittance function, $Z(\omega_{2mk}, \phi, \lambda)$, from maps of the in-phase and quadrature components.

$$Z(\omega_{2mk}, \phi, \lambda) = X(\omega_{2mk}, \phi, \lambda) + iY(\omega_{2mk}, \phi, \lambda) = \frac{\zeta^i(\omega_{2mk}, \phi, \lambda) - i\zeta^o(\omega_{2mk}, \phi, \lambda)}{(-1)^{m+\delta_{0m}} |H_{2mk}|} \tag{A4}$$

[52] Step 3: Solve for maps of the complex convolution weights, $U_{2m}(\phi, \lambda, s) = u_{2m}(\phi, \lambda, s) + iv_{2m}(\phi, \lambda, s)$, by applying equation (10) to the admittance maps of the K tidal components, where a reasonable value for τ in the diurnal and semidiurnal band is 2 days.

[53] Step 4: Decompose the maps of the convolution weights into their spherical harmonic components, as shown

in equation (12), to derive the normalized complex spherical harmonic coefficients, $D_{lp}^{2m}(s)$ and $E_{lp}^{2m}(s)$.

[54] Equation (10) defines the smooth admittance function with $(2S + 1)$ complex coefficients, and is therefore solved exactly when there are $K = 2S + 1$ tidal components available to derive the convolution weights. As such, K should be odd-valued to exactly fit the available tidal components, in which case the limit on the Fourier series is defined by $S = (K - 1)/2$.

[55] **Acknowledgments.** The work described in this paper was performed at the Jet Propulsion Laboratory, California Institute of Technology, under a contract with the National Aeronautics and Space Administration. The authors thank Richard Ray and Fabien Lefèvre for use of their ocean tide models, GOT00.2 and FES2004, respectively. We thank Srinivas Bettadpur for providing us with the GRACE baseline goals and GGM02C performance data. Our thanks also to the reviewers for their helpful comments.

References

Bettadpur, S. V., and R. J. Eanes (1994), Geographical representation of radial orbit perturbations due to ocean tides: Implications for satellite altimetry, *J. Geophys. Res.*, *99*(C12), 24,883–24,892.

Cartwright, D. E., and A. C. Edden (1973), Corrected tables of tidal harmonics, *Geophys. J. R. Astron. Soc.*, *33*, 253–264.

Cartwright, D. E., and R. D. Ray (1990), Oceanic tides from Geosat altimetry, *J. Geophys. Res.*, *95*(C3), 3069–3090.

Cartwright, D. E., and R. J. Taylor (1971), New computations of the tide-generating potential, *Geophys. J. R. Astron. Soc.*, *23*, 45–74.

Casotto, S. (1993), The mapping of Kaula's solution into the orbital reference frame, *Celest. Mech.*, *55*, 223–241.

Cheng, M. K. (2002), Gravitational perturbation theory for intersatellite tracking, *J. Geod.*, *76*, 169–185.

Desai, S. D. (2002), Observing the pole tide with satellite altimetry, *J. Geophys. Res.*, *107*(C11), 3186, doi:10.1029/2001JC001224.

Desai, S. D., and J. M. Wahr (1995), Empirical ocean tide models estimated from TOPEX/POSEIDON altimetry, *J. Geophys. Res.*, *100*(C12), 25,205–25,228.

Doodson, A. T. (1921), The harmonic development of the tide-generating potential, *Proc. R. Soc. London, Ser. A*, *100*, 305–329.

Fu, L., E. J. Christensen, C. A. Yamarone, M. Lefebvre, Y. Ménard, M. Dorrer, and P. Escudier (1994), TOPEX/POSEIDON mission overview, *J. Geophys. Res.*, *99*(C12), 24,369–24,381.

Groves, G. W., and R. W. Reynolds (1975), An orthogonalized convolution method of tide prediction, *J. Geophys. Res.*, *80*(30), 4131–4138.

Knudsen, P. (2003), Ocean tides in GRACE monthly averaged gravity fields, *Space Sci. Rev.*, *108*, 261–270.

Knudsen, P., and O. Andersen (2002), Correcting GRACE gravity fields for ocean tide effects, *Geophys. Res. Lett.*, *29*(8), 1178, doi:10.1029/2001GL014005.

Lefèvre, F. (2002), Modélisation de la marée océanique à l'échelle globale par la méthode des éléments finis avec assimilation de données altimétriques, *CLS Tech. Memo., CLS-DOS-NT-01.416/SALP-RP-MA-21060-CLS*.

Lemoine, F. G., et al. (1998), The development of the joint NASA GSFC and NIMA geopotential model EGM96, *NASA Tech. Rep., 1998-206861*.

Le Provost, C., F. Lyard, and J.-M. Molines (1991), Improving ocean tide predictions by using additional semidiurnal constituents from spline interpolation in the frequency domain, *Geophys. Res. Lett.*, *18*(5), 845–848.

McCarthy, D. D., and G. Petit (Eds.) (2004), IERS Conventions (2003), *Int. Earth Rotation Ref. Syst. Serv. (IERS), Tech. Note 32*.

Munk, W. H., and D. E. Cartwright (1966), Tidal spectroscopy and predictions, *Philos. Trans. R. Soc. London, Ser. A*, *259*, 533–581.

Ray, R. D. (1999), A global ocean tide model from TOPEX/POSEIDON altimetry: GOT99.2, *NASA Tech. Memo., 209478*.

Ray, R. D., and D. E. Cartwright (1994), Satellite altimeter observations of the Mf and Mm ocean tides, with simultaneous orbit corrections, in *Gravimetry and Space Techniques Applied to Geodynamics and Ocean Dynamics*, *Geophys. Monogr. Ser.*, vol. 82, edited by B. E. Schutz et al., pp. 69–78, AGU, Washington, D. C.

Ray, R. D., and G. D. Egbert (2004), The global S1 tide, *J. Phys. Oceanogr.*, *34*, 1922–1935.

Ray, R. D., D. D. Rowlands, and G. D. Egbert (2003), Tidal models in a new era of satellite gravimetry, *Space Sci. Rev.*, *108*, 271–282.

Shum, C. K., et al. (1997), Accuracy assessments of recent global ocean tide models, *J. Geophys. Res.*, *102*(C11), 25,173–25,194.

Standish, E. M. (1998), JPL Planetary and Lunar Ephemerides, DE405/LE405, *Interoff. Memo. 312.F-98-048*, Jet Propul. Lab., Pasadena, Calif.

Tamura, Y. (1987), A harmonic development of the tide-generating potential, *Bull. Inf. Marees Terr.*, *99*, 6813–6855.

Tapley, B. D., S. Bettadpur, J. C. Ries, P. F. Thompson, and M. M. Watkins (2004a), GRACE measurements of mass variability in the Earth system, *Science*, *305*(5683), 503–505.

Tapley, B. D., S. Bettadpur, M. Watkins, and C. Reigber (2004b), The gravity recovery and climate experiment: Mission overview and early results, *Geophys. Res. Lett.*, *31*, L09607, doi:10.1029/2004GL019920.

Thompson, P. F., S. V. Bettadpur, and B. D. Tapley (2004), Impact of short period, non-tidal, temporal mass variability on GRACE gravity estimates, *Geophys. Res. Lett.*, *31*, L06619, doi:10.1029/2003GL019285.

Wahr, J., and T. Sasao (1981), A diurnal resonance in the ocean tide and in the Earth's load response due to the resonant free 'core nutation', *Geophys. J. R. Astron. Soc.*, *64*, 747–765.

Wahr, J., M. Molenaar, and F. Bryan (1998), Time variability of the Earth's gravity field: Hydrological and oceanic effects and their possible detection using GRACE, *J. Geophys. Res.*, *103*(B12), 30,205–30,229.

Wahr, J., S. Swenson, V. Zlotnicki, and I. Velicogna (2004), Time-variable gravity from GRACE: First results, *Geophys. Res. Lett.*, *31*, L11501, doi:10.1029/2004GL019779.

Zetler, B. D., and W. H. Munk (1975), The optimal wiggliness of tidal admittances, *J. Mar. Res. Suppl.*, *33*, 1–13.

S. D. Desai and D.-N. Yuan, Jet Propulsion Laboratory, M/S 238-600, 4800 Oak Grove Drive, Pasadena, CA 91109, USA. (shailen.desai@jpl.nasa.gov)